

# Optical Resonance and Near-Field Effects: Applications for Nanopatterning

B. S. Luk'yanchuk<sup>a,\*</sup>, Z.B. Wang<sup>a,b</sup>, M.H. Hong<sup>a,b</sup>, T.C. Chong<sup>a</sup>, and N. Arnold<sup>c</sup>

<sup>a</sup>Data Storage Institute, DSI Building, 5 Engineering Drive 1, Singapore 117608, Republic of Singapore

<sup>b</sup>Department of Electrical and Computer Engineering, National University of Singapore,  
Singapore 117576, Republic of Singapore

<sup>c</sup>J. Kepler Universitaet Linz, Institut fuer Angewandte Physik, A-4040 Linz, Austria

## ABSTRACT

A spherical particle can be used as a lens for focusing laser radiation. It has potential applications in high-density data storage and high-resolution optical lithography for nano-device fabrication

PACS: 81.16.Rf; 81.65.Cf

## 1. INTRODUCTION

The problem of electromagnetic field scattering by a spherical particle has an exact solution given by the Mie theory [1]. This solution demonstrates that a small transparent particle can work as a near-field lens, which leads to a strong field enhancement. In the vicinity of the particle the flux of energy is localized in the area below the diffraction limit. It is attractive for many applications in optical recording and surface nanopatterning [2-20]. In the present paper we discuss some peculiarities of light scattering for three types of particles: a transparent particle, a particle with surface plasmon resonance and a particle with negative refractive index. The fine structure of the field for a particle situated near the surface is also discussed.

## 2. A TRANSPARENT PARTICLE

Geometrical optics [21] yields the simplest approach to understanding the energy flux within the weakly absorbing media. This approach is applicable for particles (radius  $a$ ) with a size significantly larger than the radiation wavelength, e.g.,  $a \gg \lambda$ . In this case the intensity distribution around the particle can be estimated using ray tracing according to Snell's law and energy conservation. For a particle with refractive index  $1 < n < 2$  in vacuum, the refracted rays form a caustic under the particle, see the example in Fig. 1.

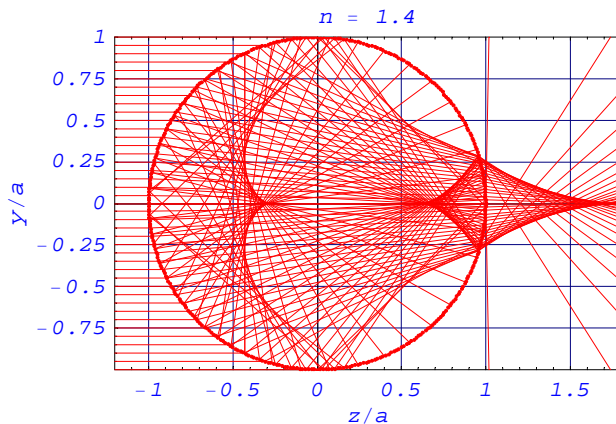


**Fig. 1.** Ray tracing for a big particle  $a \gg \lambda$  with refractive index  $n = 1.4$ . The incidence angle  $\theta_i$  and the refraction angle  $\theta_t$  inside the sphere are related by  $\theta_t = \arcsin[\sin\theta_i / n]$ . Upon second refraction the ray leaves the sphere at a point with the polar angle with the  $z$ -axis  $\theta_o = 2\theta_t - \theta_i$ , and emerges from the sphere in the direction  $\theta_{ou} = 2\theta_t - 2\theta_i < 0$ . The caustic crosses the sphere at the angle  $\theta_{om}$  given by the condition  $\sin^2 \theta_{om} = (4 - n^2)^3 / 27n^4$ . The Corresponding angle of incidence  $\theta_{im}$  is given by  $\sin^2 \theta_{im} = (4 - n^2) / 3$ . We approximate the spot size on the substrate by caustic on the sphere:  $w_g \approx a \sin \theta_{om}$ .

\* [Boris\\_LUKIYANCHUK@dsi.a-star.edu.sg](mailto:Boris_LUKIYANCHUK@dsi.a-star.edu.sg) ; Phone: (65) 6874 8702; fax: (65) 6777 1349

Geometrical optics approximation yields the estimation for intensity enhancement factor under the particle [22, 23]:

$$\frac{I_m}{I_0} \approx \frac{a^2}{w_g^2} \approx \frac{27n^4}{(4-n^2)^3}. \quad (1)$$

Because of diffraction and aberrations the structure of the field is more complicated than it follows from Fig. 1. Under some approximations this fine field structure for a big particle can be presented by a Bessoid integral [24]

$$J(x, z) = \int_0^{\infty} J_0(xt) t \exp[i(t^4 + zt^2)] dt. \quad (2)$$

With a similar approximation the field scattered by a cylindrical lens is given by a Pearcey integral [25]

$$\Psi(x, z) = \int_{-\infty}^{\infty} dt \exp[i(t^4 + zt^2 + xt)]. \quad (3)$$

Here  $J(x, z)$  and  $\Psi(x, z)$  are complex functions of two normalized variables, while intensity is considered to be square modulus of these functions. The path of integration in (2) and (3) is such that the integrands vanish at its terminal points at infinity. The intensity distributions, presented by these functions (see e.g. Fig. 1 in [24] and Fig. 1 in [25]) are qualitatively similar to those, which follow from the solution of the wave equation for the cylinder [26] and sphere [27]. The contour plot of the integral (2) is shown in Fig. 2. The peculiarity of the diffraction pattern for the spherical particle is an additional caustic line along the  $z$ -axis [23, 27]. This caustic is responsible for the maximal laser intensity under the particle. Naturally, more detailed calculations of the field structure should be based on the Mie theory. An example of these calculations is shown in Fig. 3. It confirms the “Bessoid structure” of the field distribution within the caustic region.

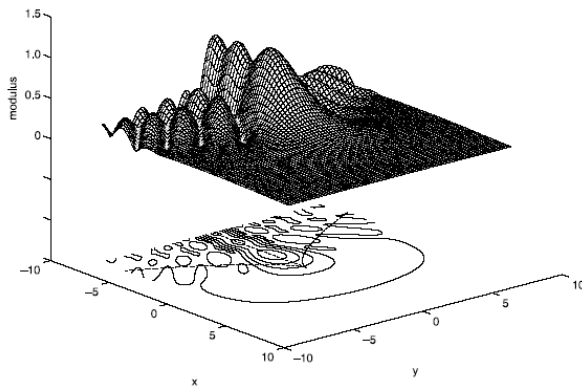


Fig. 2. Field distribution, which follows from the Bessoid integral (2). Perspective and contour plots of  $|J(x, y)|$  according [24].

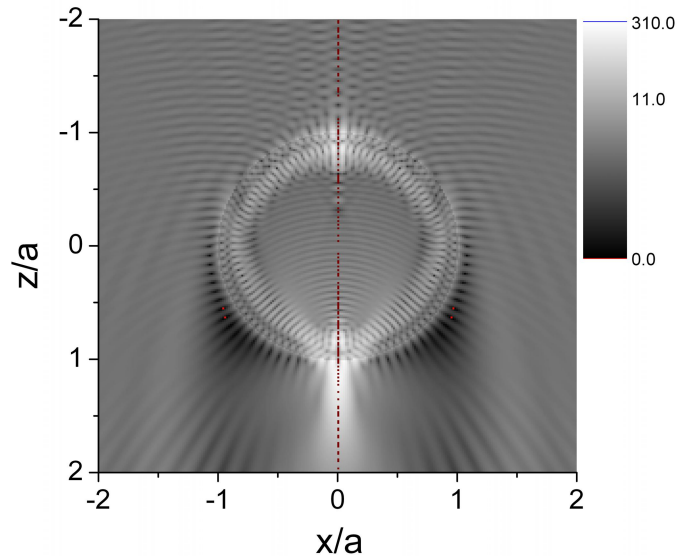


Fig. 3. Field distribution,  $I = E^2$ , calculated from the Mie theory for spherical particle  $a = 1.5 \mu\text{m}$  with refraction index  $n = 1.5$ ,  $\lambda = 248 \text{ nm}$ . Intensity is shown in logarithmic scale, which presents the region of geometrical shadow better (dark region under the particle). Near the output edge of the particle one can clearly see the typical “Bessoid structure” of the intensity distribution.

The fine field structure in the near-field region demonstrates the field localization beyond the diffraction limit. One can see in Fig. 3 about 100 bright rays around the particle, which means that the average size of each ray is about 100 nm. This effect can be used for nanopatterning of the surface. It was confirmed experimentally [2-20], that the spherical particle situated on the surface of the material permits to create material modification or even ablation within the range of 100 nm. To analyze this effect more precisely, Mie theory is insufficient, because it does not take into account the secondary scattering of radiation, reflected from the surface. The theory of a particle on the surface was developed in [28]. It also presents the exact solution of the wave equation with corresponding boundary conditions.

We applied this solution for laser cleaning problem in [2, 27]. Practical usage of this solution needs however long calculation time, related to the calculation of Weyl type integrals within the matrix, which describes the reflection of the spherical wave:

$$\Pi_{\ell}^m(r) = \frac{i^{-\ell}}{2\pi} \int_0^{2\pi} d\beta \int_0^{\pi/2-i\infty} d\alpha \sin\alpha e^{ikr\cos\gamma} Y_{\ell}^m(\alpha, \beta), \quad (4)$$

where  $Y_{\ell}^m(\alpha, \beta)$  are the spherical harmonics, related to associate Legendre polynomials. We have used the FORTRAN program, which permits to do calculations in reasonable time.

In spite of the difficulties with the numerical calculation, the situation is rather clear from the physical point of view. Qualitatively the substrate surface works like a mirror coupled with a spherical resonator (particle); it should lead to an increase in optical enhancement and decrease in the area of the field localization (sharpening effect). This effect is confirmed by calculations. In Fig. 4 the intensity distribution within the  $x$ - $z$  plane is shown; one can see enhanced radiation intensity, which came through the transparent particle after its reflection by the surface. This effect may play a role for enhanced Raman scattering.

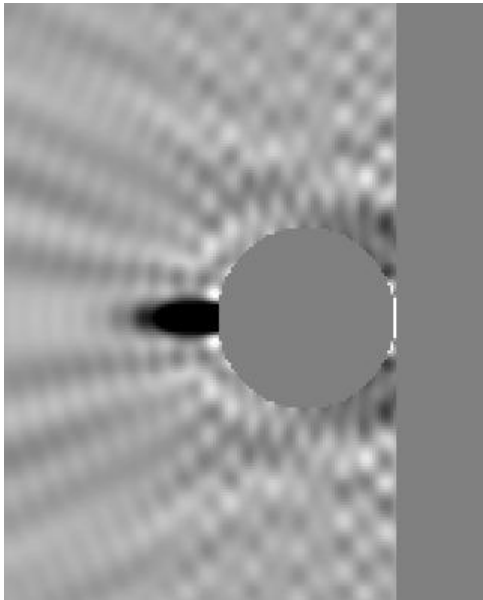


Fig. 4. The intensity distribution ( $z$ -component of the Poynting vector) within the  $x$ - $z$  plane for radiation with  $\lambda = 248$  nm, scattered by polystyrene particle ( $n = 1.6$ ,  $a = 0.5 \mu\text{m}$ ) on Si surface. Gradations of the intensity are given from negative (dark) to positive (light) values. The dark area on the top of the particle corresponds to an energy flux directed up, while the white area under the particle corresponds to energy flux directed to the substrate.

All the mentioned above papers [2-20] use the main maximum in the intensity distribution under the particle to produce the surface nanopatterning. The produced nanostructures were formed with a normal incidence wave at positions where spheres originally locate. However in Fig. 3 one can see the majority of additional rays in a directional pattern. Although these rays are of smaller intensity the field localization for a minor lobe can be even higher than for the main lobe. It can be clearly seen from the picture of Bessoid integral in Fig. 2. This fine structure should be developed with the angular incidence wave.

Calculations, presented in Fig. 5 show intensity distribution under the polysterene (PS) particle with diameter  $2a = 1 \mu\text{m}$  on the surface of GeSbTe (GST) film for radiation of KrF excimer laser ( $\lambda = 248$  nm). One can see from the figure that a fine structure is developed at incident illumination of the particle in the form of “comet shape” ring nanostructure, which consists of small dots around the particle.

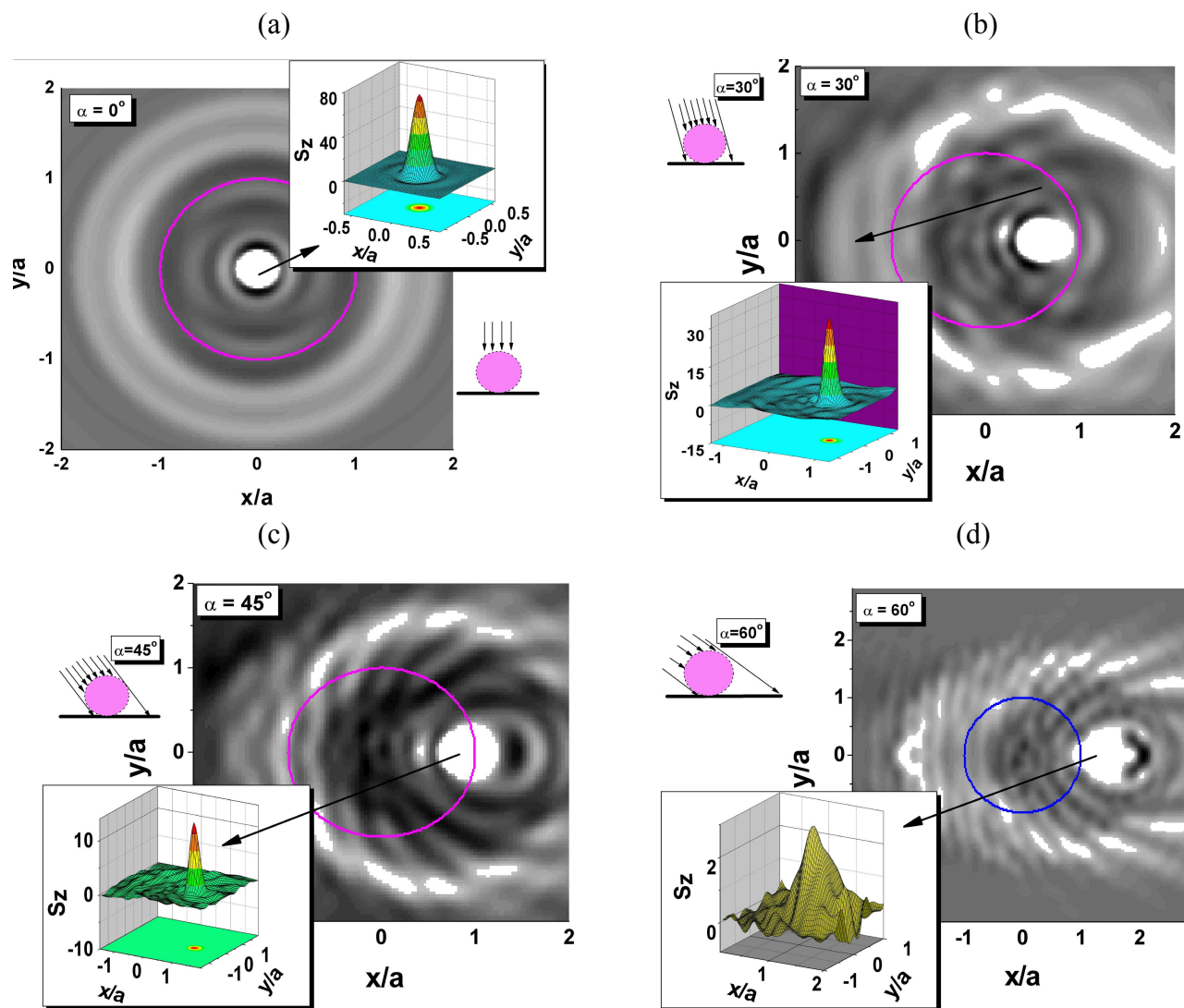


Fig. 5. Calculated intensity distribution ( $z$  - component of the Poynting vector) under  $1.0 \mu\text{m}$  PS particles at different incidence angles of (a)  $\alpha = 0^\circ$ , (b)  $\alpha = 30^\circ$ , (c)  $\alpha = 45^\circ$  and (d)  $\alpha = 60^\circ$  respectively. The white color represents the areas where the intensity field exceeded the material damage threshold  $12.0 \text{ mJ/cm}^2$ . Surface thermal deformation is neglected.

This structure was found experimentally in [29]. An example of this experiment is shown in Fig. 6. This structure is in a good agreement with theoretical calculations in Fig. 5. The origin of this effect is related to Bessel structure of the intensity, modified by secondary scattering effects.

In conclusion we have to say that the transparent particles with the size by the order of the radiation wavelength can be used as a near-field lens for nanopatterning on the scale about  $100 \text{ nm}$ . Different modifications of this technique can be used in applications. For example, the self-assembled array of particles can be used for this nanopatterning [8-12, 19, 20]. Another idea is to use particles as a mask for projection photolithography [14, 30, 31]. This scheme permits to utilize the interference effects from the focused beams under the particles [14, 32]. There are many other techniques for nanopatterning which use transparent particles and their combination with etching, deposition or surface modification processes [15, 33].

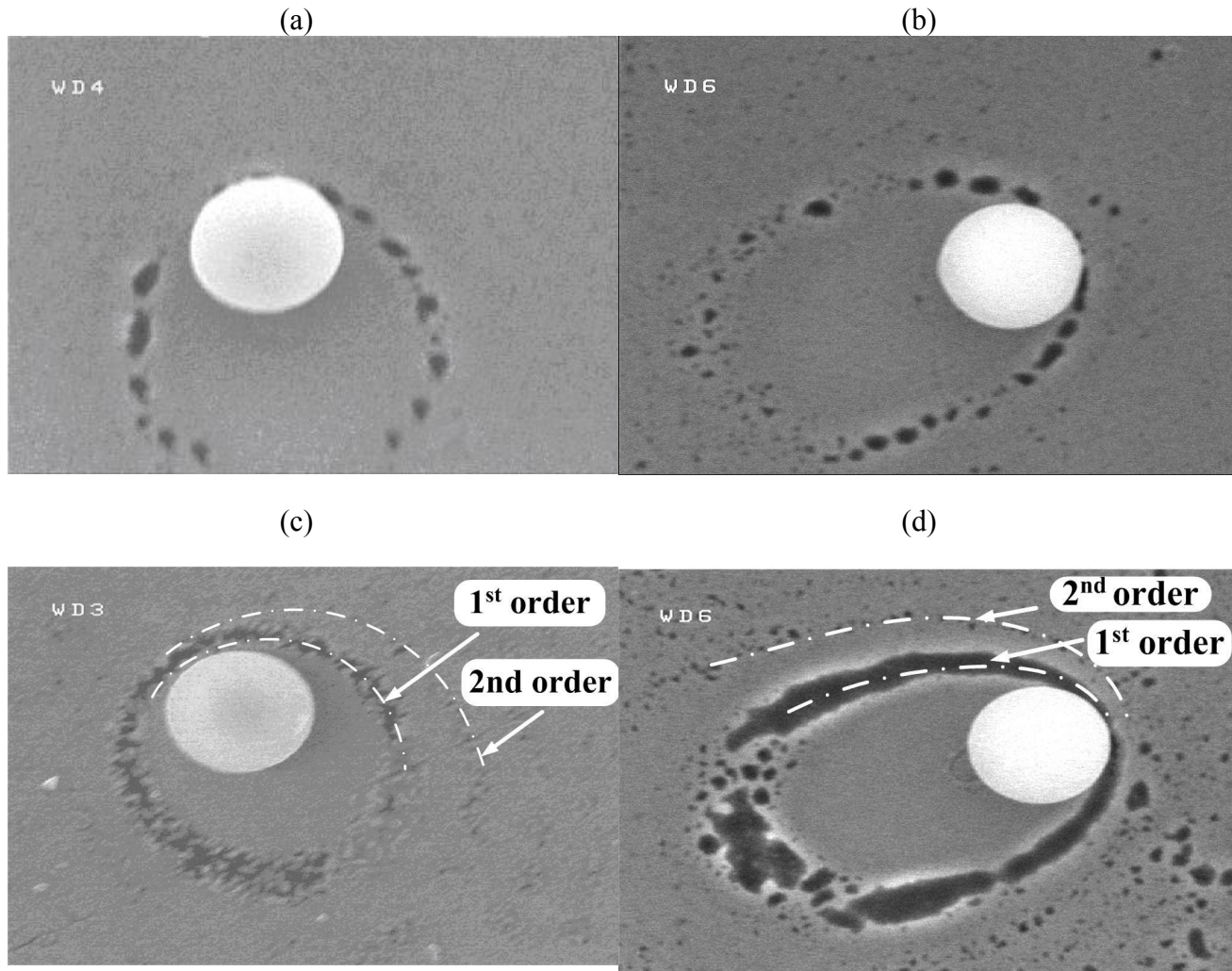


Fig. 6. SEM images of comet-shape patterns formed on GST film around un-removed particles at different angles and laser fluences, (a)  $\alpha = 45^\circ$ ,  $7.5 \text{ mJ/cm}^2$ , (b)  $\alpha = 60^\circ$ ,  $7.5 \text{ mJ/cm}^2$ , (c)  $\alpha = 45^\circ$ ,  $10.5 \text{ mJ/cm}^2$  and (d)  $\alpha = 60^\circ$ ,  $10.5 \text{ mJ/cm}^2$ . The dashed lines show different orders of the rings. The diameter of PS sphere is  $1.0 \mu\text{m}$ . KrF excimer pulsed laser ( $\lambda=248 \text{ nm}$ , FWHM = 23 ns) was used as a light source.

### 3. A PARTICLE WITH SURFACE PLASMON RESONANCE

Another interesting idea is to use the metallic nanoparticles for nanopatterning [16, 34]. This kind of particles should produce the outward flux of energy in the near-field region. To understand the applicability of this method, one should analyze the energy flux around the metallic particle. At dipole approximation the whole energy flux enters into the particle [35]. At the same time dipole approximation can be inadequate for the problem with small dissipation [36]. The latter is related to inverse transformation of surface plasmons generated in the particle by the incident light into the scattered electromagnetic field [36]. Recently this problem was investigated in [37] on the basis of the Mie theory. For the case of surface plasmon excitation, when  $\text{Re} \epsilon = -2$  ( $\epsilon$  is the dielectric function), the energy flux for small size parameter  $q = 2\pi a/\lambda \ll 1$  demonstrates quite complicated behavior, depending on dissipation factor,  $\text{Im} \epsilon$ . The non-dissipative damping leads to fascinating peculiarities in the scattered field, e.g. formation of optical vortices, etc., see in Fig. 7.

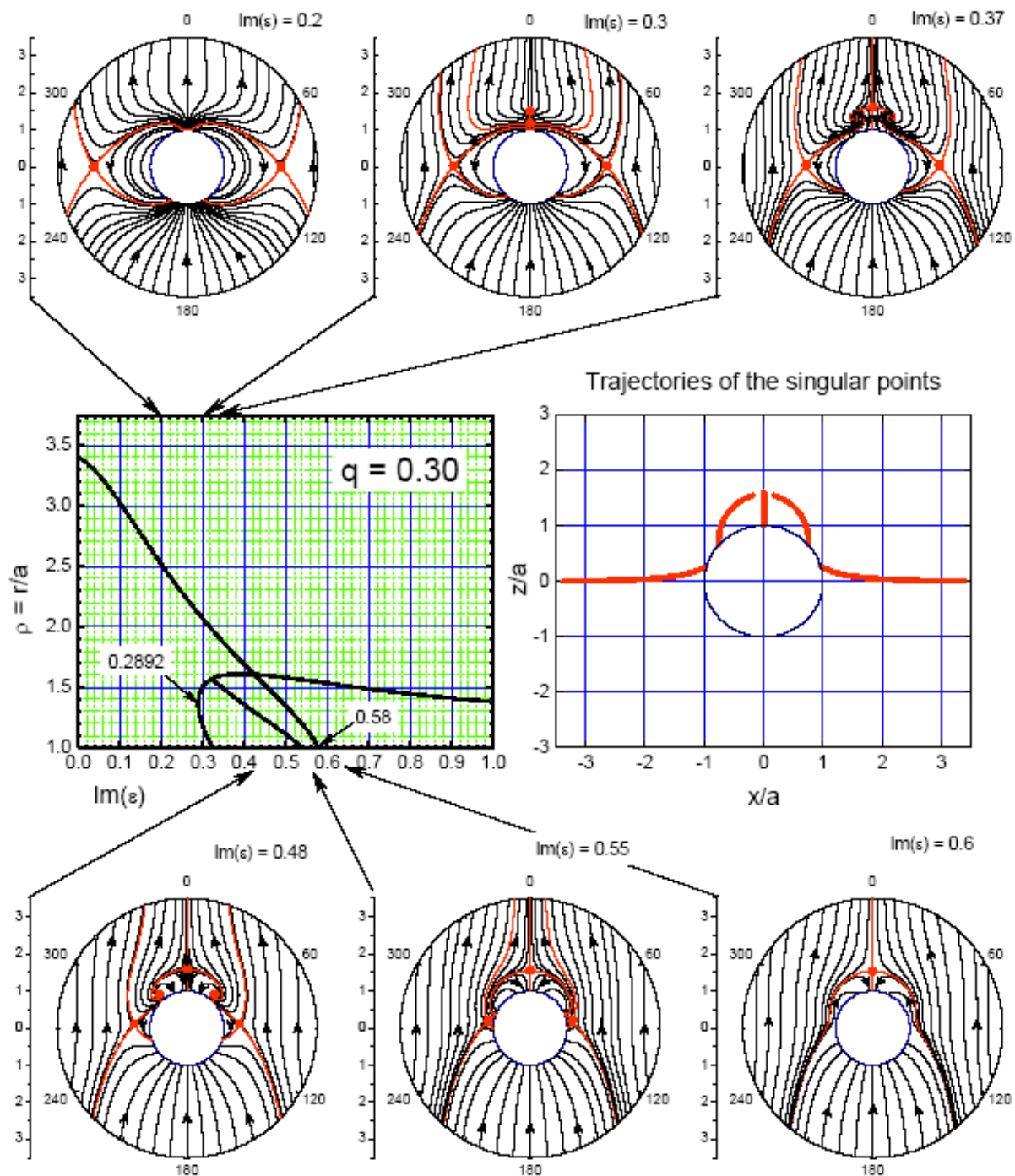


Fig. 7. Field lines in  $xz$ -plane for a particle with plasmon resonance  $\text{Re } \epsilon = -2$  and size parameter  $q = 0.3$ . Central part of the picture presents stationary points and their trajectories versus  $\text{Im } \epsilon$ .

The field of the surface plasmon is localized very close to the nanoparticle surface. For example in Fig. 8 the distribution of electric field is shown for Ag particle with size  $a = 5$  nm. When similar particles closely situated energy flux demonstrates efficient coupling [38]. This permits to realize nanoparticle chain waveguides [39]. Less investigated is coupling of the plasmon nanoparticle with a surface, although this coupling plays an important role for super resolution optical disk technology [40]. The field of nanoparticles situated on the surface can be used for nanopatterning. It was experimentally demonstrated in [16, 34].

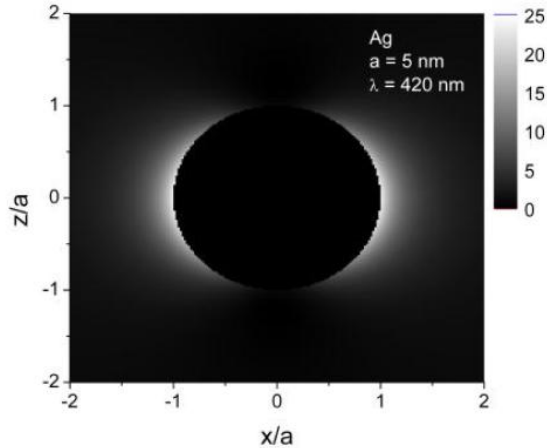


Fig. 8. Contour plot for distribution of electrical field  $E^2$  around a silver particle illuminated by radiation with  $\lambda = 420$  nm. Polarization corresponds to electrical vector directed along x-coordinate. Localized surface plasmon clearly indicated the shape typical for dipole excitation.

#### 4. A PARTICLE WITH NEGATIVE REFRACTIVE INDEX

In 1968 V. Veselago suggested the idea of materials with a negative refractive index [41]. Recently it was shown that media with a negative refraction index can be realized on the base of special composite materials [42]. This discovery leads to a great number of publications (one can find about 200 references on the site of Prof. Veselago [43]). Media with a negative refractive index (the so called left-handed materials) has some unusual physical properties, which are attractive for many applications. For example, J. Pendry suggested the media with a negative refractive index as a perfect lens [44].

Although these materials were realized for SHF diapason with frequencies about 10 GHz, many people believe that it would be possible to realize media with a negative refractive index in optical region. Thus we analyzed theoretically the ability to use these materials for near-field patterning. In Fig. 9 and 10 the contour plots for intensity distributions are shown for materials with a negative refractive index. Calculations were performed on the basis of the Mie theory. For comparison we show both: materials with a positive and a negative refractive index. One can see different bending of the wave fronts and completely different caustics under the particles. A particle with a negative  $n$  in Fig. 10 produces a complex circular pattern in the near field region.

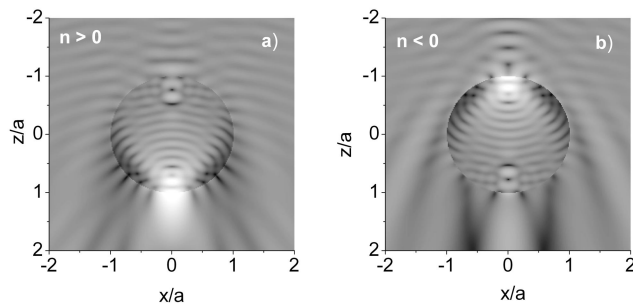


Fig. 9. Contour plot for distribution of electrical field  $E^2$  inside and around the particle with radius  $a = 0.5$   $\mu\text{m}$  illuminated by radiation with  $\lambda = 248$  nm. Electrical vector directed along x - coordinate. For left picture  $n = 1.6$  (a) and for right picture  $n = -1.6$  (b).

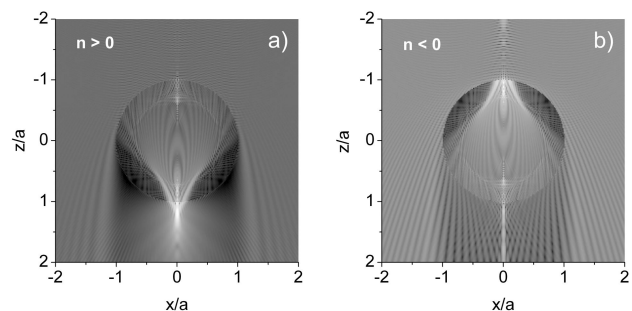


Fig. 10. The same as in Fig. 9, but for the particle with size  $a = 5$   $\mu\text{m}$ .

## REFERENCES

1. M. Born, E. Wolf: *Principles of Optics*, 7-th Edition, (Cambridge University Press, 1999)
2. B. S. Luk'yanchuk, Y. W. Zheng, Y. F. Lu: *Proc. SPIE*, vol. **4065**, 576 (2000)
3. Y. F. Lu, L. Zhang, W. D. Song, Y. W. Zheng, B. S. Luk'yanchuk: *JETP Lett.* **72**, 457 (2000)
4. H.-J. Münzer, M. Mosbacher, M. Bertsch, J. Zimmerman, P. Leiderer, J. Bonneberg: *J. Microscopy* **202**, 129 (2001)
5. L. Zhang, Y. F. Lu, W. D. Song, Y. W. Zheng, B. S. Luk'yanchuk: *MRS Proceedings*, vol. **676**, pp. Y 4.3 (2001)
6. M. Mosbacher, H.-J. Münzer, J. Zimmermann, J. Solis, J. Boneberg, P. Leiderer: *Appl. Phys. A* **72**, 41 (2001)
7. Y. F. Lu, L. Zhang, W. D. Song, Y. W. Zheng, B. S. Luk'yanchuk: *Proc. SPIE*, vol. **4426**, 143 (2002)
8. H.-J. Münzer, M. Mosbacher, M. Bertsch, O. Dubbers, A. Pack, R. Wannemacher, B.-U. Runge, D. Bäuerle and P. Leiderer: *Proc. SPIE*, vol. **4426**, 180 (2002)
9. B. S. Luk'yanchuk, M. Mosbacher, Y. W. Zheng, H.-J. Münzer, S. M. Huang, M. Bertsch, W. D. Song, Z. B. Wang, Y. F. Lu, O. Dubbers, J. Boneberg, P. Leiderer, M. H. Hong, T. C. Chong: Chapter 3 in "Laser cleaning", B. S. Luk'yanchuk (Ed.), (World Scientific, New Jersey, London, Singapore, Hong Kong, 2002)
10. S. M. Huang, M. H. Hong, B. S. Luk'yanchuk, Y. F. Lu, W. D. Song, T. C. Chong: *J. Vacuum and Sci. Tech.* **B 20**, 1118 (2002)
11. S. M. Huang, M. H. Hong, Y. F. Lu, B. S. Luk'yanchuk, W. D. Song, T. C. Chong: *J. Appl. Phys.* **92**, 2495 (2002)
12. S. M. Huang, M. H. Hong, B. Luk'yanchuk, Y. F. Lu : *Proc. SPIE*, vol. **4760**, 185 (2002)
13. K. Piglmayer, R. Denk, D. Bäuerle: *Appl. Phys. Lett.* **80**, 4693 (2002)
14. R. Denk, K. Piglmayer, D. Bäuerle: *Appl. Phys. A* **76**, 1 (2003)
15. R. Denk, K. Piglmayer, D. Bäuerle: *Appl. Phys. A* **76**, 549 (2003)
16. S. M. Huang, B. S. Luk'yanchuk, M. H. Hong, T. C. Chong: *Appl. Phys. Lett.* **82**, 4809 (2003)
17. F. Lang, M. Mosbacher, P. Leiderer: *Appl. Phys. A* **77**, 117 (2003)
18. S. M. Huang, M. H. Hong, B. Luk'yanchuk, Z. B. Wang: *Appl. Phys. A* **77**, 293 (2003)
19. M. H. Hong, S. M. Huang, B. Luk'yanchuk, Z. B. Wang, Y. F. Lu, T.C. Chong: *Proc. SPIE*, vol. **4977**, 142 (2003)
20. M.H. Hong, S. M. Huang, B. Luk'yanchuk, T.C. Chong: *Sensors and Actuators A-Physical*, vol. **108**, 69 (2003)
21. Yu. A. Kravtsov, Yu. I. Orlov, *Geometrical Optics of Inhomogeneous Media* (Springer, Berlin, 1990).
22. N. Arnold: *Appl. Surf. Sci.* **208-209**, 15 (2003)
23. B. S. Luk'yanchuk, N. Arnold, S. M. Huang, Z. B. Wang, M. H. Hong: *Appl. Phys. A* **77**, 209 (2003).
24. N. P. Kerk, J. N. L. Connor, P. R. Curtis, C. A. Hobbs: *J. Phys. A: Math. Gen.* **33**, 4797 (2000)
25. J. F. Nye: *J. Opt. A: Pure Appl. Opt.* **5**, 495 (2003)
26. W. Zalowich: *Phys. Rev. E.* **64**, 066610 (2001)
27. B. S. Luk'yanchuk, Z. B. Wang, W. D. Song, M. H. Hong: *Appl. Phys. A* **79**, (2004)
28. P. A. Bobbert, J. Vlieger: *Physica A* **137**, 209 (1986)
29. Z. B. Wang, M.H. Hong, B. S. Luk'yanchuk, Y. Lin, Q. F. Wang, T.C. Chong, submitted to *J. Appl. Phys.*
30. M. H. Lu, G. M. Whitesides: *Appl. Phys. Lett.* **78**, 2273 (2001)
31. M. H. Lu, G. M. Whitesides: *Appl. Phys. Lett.* **80**, 3500 (2002)
32. D. Bäuerle, K. Piglmayer, R. Denk, N. Arnold: *Lambda Highlights*, No. **60** (2002)
33. G. Wysocki, R. Denk, K. Piglmayer, N. Arnold, D. Bäuerle: *Appl. Phys. Lett.* **82**, 692 (2003)
34. P. G. Kik, S. A. Maier, H. A. Atwater: *Mat. Res. Soc. Symp. Proc.* **705**, Y3.6 (2002)
35. C. F. Bohren, *J. Phys.* **51**, 323 (1983)
36. M. I. Tribelsky: *Sov. Phys. JETP* **59**, 534 (1984)
37. Z. B. Wang, B. S. Luk'yanchuk, M. H. Hong, Y. Lin, T. C. Chong: *Phys. Rev. B.* **70**, 032427 (2004)
38. H. X. Xu: *Phys. Lett. A* **312**, 411 (2003)
39. S. A. Maier, P. G. Kik, H. A. Atwater: *Phys. Rev. B* **67**, 205402 (2003)
40. W. C. Liu, D. P. Tsai: *Jpn. J. Appl. Phys.* **42**, 1031 (2003)
41. V. Veselago: *Sov. Physics Uspekhi* **10**, 509 (1968)
42. R. A. Shelby, D. R. Smith, S. Shultz: *Science* **292**, 77 (2001)
43. V. Veselago: <http://zhurnal.ape.relarn.ru/~vgv/>
44. J. B. Pendry: *Phys. Rev. Lett.* **85**, 3966 (2000)